Pflugers Arch - Eur J Physiol (2011) 462:733–743
DOI 10.1007/s00424-011-1020-8

SIGNALING AND CELL PHYSIOLOGY

In vivo key role of reactive oxygen species and NHE-1 activation in determining excessive cardiac hypertrophy

Oscar H. Cingolani · Néstor G. Pérez · Irene L. Ennis · María C. Álvarez · Susana M. Mosca · Guillermo R. Schinella · Eduardo M. Escudero · Gloria Cónsole · Horacio E. Cingolani

Received: 3 June 2011 / Revised: 12 August 2011 / Accepted: 12 August 2011 / Published online: 26 August 2011

Abstract Growing in vitro evidence suggests NHE-1, a known target for reactive oxygen species (ROS), as a key mediator in cardiac hypertrophy (CH). Moreover, NHE-1 inhibition was shown effective in preventing CH and failure; so has been the case for AT1 receptor (AT1R) blockers. Previous experiments indicate that myocardial stretch promotes angiotensin II release and post-translational NHE-1 activation; however, in vivo data supporting this mechanism and its long-term consequences are scanty. In this work, we thought of providing in vivo evidence linking AT1R with ROS and NHE-1 activation in mediating CH. CH was induced in mice by TAC. A group of animals was treated with the AT1R blocker losartan. Cardiac contractility was assessed by echocardiography and pressure–volume loop hemodynamics. After 7 weeks, TAC increased left ventricular (LV) mass by ~45% vs. sham and deteriorated LV systolic function. CH was accompanied by activation of the redox-sensitive kinase $p90^{RSK}$ with the consequent increase in NHE-1 phosphorylation. Losartan prevented $p90^{RSK}$ and NHE-1 phosphorylation, ameliorated CH and restored cardiac function despite decreased LV wall thickness and similar LV systolic pressures and diastolic dimensions (increased LV wall stress). In conclusion, AT1R blockade prevented excessive oxidative stress, $p90^{RSK}$ and NHE-1 phosphorylation, and decreased CH independently of hemodynamic changes. In addition, cardiac performance improved despite a higher work load.

Keywords Hypertrophy · Sodium–hydrogen exchange · Oxidative stress · Angiotensin · Phosphorylation

O. H. Cingolani (✉)
Division of Cardiology, Johns Hopkins University Hospital,
720 Rutland Avenue, Ross 835,
Baltimore, MD 21205, USA
e-mail: ocingol1@jhmi.edu

N. G. Pérez · I. L. Ennis · M. C. Álvarez · S. M. Mosca · G. R. Schinella · E. M. Escudero · G. Cónsole · H. E. Cingolani
Centro de Investigaciones Cardiovasculares,
Facultad de Ciencias Médicas, Universidad Nacional de La Plata,
Calle 60 y 120,
1900, La Plata, Argentina

Introduction

Cardiac hypertrophy (CH) is known as one of the main cardiovascular risk factors and a poor prognostic sign associated with nearly all forms of heart failure [27, 32]. Most intracellular pathways leading to pathological CH converge at the increase in intracellular calcium levels and the downstream calcineurin-dependent transcriptional pathway. This rise in calcium may occur through different mechanisms. One of them is the increase in intracellular Na^+ resulting from enhanced function of the NHE-1, which drives the Na^+/Ca^{2+} exchanger to increase the Ca^{2+} transient. After cardiac muscle is stretched, an autocrine/paracrine chain of steps occur in which angiotensin II (AII) mediated AT1 receptor (AT1R) activation is an early event [44]. This pathway also involves NADPH oxidase (NOX)-dependent mitochondrial reactive oxygen species (ROS) release, which itself activates the $p90^{RSK}$ -NHE-1 redox-sensitive kinase, among others (for review, see Ref. [22]). Recently, Nakamura et al. [40] demonstrated in vitro that NHE-1 hyperactivity is sufficient to generate Ca^{+2} signals required for CH to take place. However, in vivo physiological data supporting the involvement of this mechanism in the transition to chronic CH and its consequences is scant.

Enhanced NHE-1 activity as a possible mechanism responsible of CH and failure was previously reported in

the hypertrophic myocardium of adult spontaneously hypertensive rats [41]; in human ventricular myocytes from hearts with chronic end-stage heart failure [56]; in a pressure–volume overload model of CH and failure in rabbits [3]; in the hypertrophied heart of a type 2 diabetic rat model [17, 40]; and in neonatal rats [19].

Classically, pressure-overload CH is considered an adaptive mechanism by which the increase in left ventricular (LV) wall thickness normalizes wall stress. However, growing evidence is challenging this view of considering CH as a simple adaptative mechanism, by demonstrating that CH is an independent risk factor for morbidity and mortality [37]. Furthermore, a number of studies (for review, see Ref. [47]) have shown that blunting CH response to pressure overload does not result in a decrease in cardiac performance.

The aim of this work was to explore in vivo whether targeting AT1R with Losartan (LOS) will blunt ROS-mediated NHE-1 activation induced by pressure overload. Furthermore, in our CH model, achieved by transverse aortic constriction (TAC), the systemic vasodilatory effect of AT1R blockade did not significantly alter the pressure imposed to the heart (proximal to TAC), therefore allowing us to dissect this pathway, independently of LV pressure.

Methods

Animals

BALB/cAnN male mice, 8–12 weeks old, were used for the study. All procedures used during this investigation conform to the *Guide for the Care and Use of Laboratory Animals*, published by the US National Institutes of Health (NIH Publication No. 85–23, revised 1996), and to the guidelines laid down by the Animal Welfare Committee of La Plata School of Medicine (Res.13998/04).

Experimental model

TAC to induce pressure overload CH was performed using the following protocol: Anesthesia was induced with Ethomidate (10 mg kg^{-1}) and morphine (1 mg kg^{-1}), both delivered i.p. After anesthesia with 2–3% isoflurane delivered via a mechanical ventilator, the chest was shaved and opened through a small thoracic window between ribs 2 and 4, and a 26 Ga needle placed on the transverse aorta. The band was secured using a 7.0 prolene suture, the needle was then removed and the chest closed. Survival rate for this procedure was ~80%. A sham-operated group served as control. For shams, the same surgical procedure took place, except that after the aorta was exposed, no ligation was performed.

LOS (40 mg kg^{-1} day^{-1}) was given in the drinking water. This dose was selected based on previous studies in rodents from our lab as well as others [1, 24]. Treatment started 48 h before TAC surgery. All groups were followed for 7 weeks.

Physiologic studies

Cardiac function was assessed in conscious mice by transthoracic, two-dimensional, guided M-mode echocardiography (Sequoia C256, Siemens) with a 13-MHz linear-array transducer. All measurements, including LV wall thickness systolic and diastolic dimensions were performed according to the American Society of Echocardiography leading-edge method [46]. LV mass was calculated as previously described [31].

A more comprehensive in vivo cardiac mechanics analysis was performed using a miniature pressure–volume catheter (SPR-839, Millar Instruments, Inc., Houston, TX) inserted via the LV apex in anesthetized, open-chest mice as described [49]. The same anesthesia protocol (described above) for the TAC procedure was applied. Transient obstruction of the inferior vena cava was used to obtain data over a loading range.

In a separate group of mice, TAC was performed and ascending and descending aortic pressure were recorded, and gradients across the coarctation were calculated.

End-systolic, end-diastolic and peak systolic stress were calculated integrating pressure data from the hemodynamic studies and LV wall dimensions from the echo studies as previously described [20].

Assessment of lipid peroxidation

We used the thiobarbituric acid reactive substances (TBARS) spectroscopic technique to evaluate lipid peroxidation in plasma as index of ROS formation. Absorbance at 535 nm was measured and TBARS expressed in nmol/ml using an extinction coefficient of 1.56×10^{5} M^{-1} cm^{-1}.

Histological analysis

LV cardiomyocytes cross-sectional area (CSA) was determined in hematoxylin–eosine-stained slides from each heart as previously described [42]. Cardiomyocytes were accepted for quantitative analysis if: (1) their cross sections contained a centrally located nucleus and (2) the cellular membrane was unbroken. The interstitial fibrosis was assessed in picrosirius red-stained tissue slides. The percentage of collagen (collagen volume fraction [CVF]) was calculated as the sum of collagen areas divided by the total LV area (myocytes+collagen) [42].

Determination of $p90^{RSK}$ and NHE-1phosphorylation

Cardiac tissue was homogenized in lysis buffer (300 mmol/l sacarose; 1 mmol/l DTT; 4 mmol/l EGTA, protease inhibitors cocktail (Complete Mini Roche); 20 mmol/l Tris–HCl, pH 7.4). After a brief centrifugation, the supernatant was kept and protein concentration determined by the Bradford method. Samples were denatured and equal amounts of protein were subjected to PAGE and electrotransferred to PVDF membranes. Membranes were then blocked with nonfat-dry milk and incubated overnight with either anti-phospho-$p90^{RSK}$ (Cell Signaling) or anti- $p90^{RSK}$ (BD Transduction Laboratories). For NHE-1 phosphorylation determination samples were immunoprecipitated using a NHE-1 polyclonal antibody (Chemicon) and then subjected to PAGE, electrotransferred and incubated with an anti-14-3-3 binding motif antibody (Cell Signaling). Once immunoblots were assayed with the anti P-14-3-3 binding motif antibody (Cell Signaling #9601), membranes were stripped and re-assayed with a different polyclonal anti NHE-1 (Santa Cruz Biotechnology, sc-28758). The intensity of this last signal was used as a loading control. In preliminary experiments we have demonstrated that no nonspecific signal is obtained in lanes without sample. Previous reports have shown that the regulatory Ser703 of the NHE-1 lies within a sequence which creates upon phosphorylation a binding motif for 14-3-3 proteins [29, 51]. Experiments were performed in which this residue (Serine 703) of the cytosolic tail of the NHE-1 was mutated to alanine observing that only those containing $Ser(P)^{703}$ exhibited high affinity 14-3-3 binding, determining that this interaction occurs only at serine 703. Thus, the anti-P-14-3-3 binding motif antibody when probed with immunoprecipitated NHE-1 represents a useful tool to estimate NHE-1 phosphorylation at Ser703 [50]. Total $p90^{RSK}$ and NHE-1 as a loading control were assayed. Peroxidase-conjugated anti-rabbit or anti-mouse IgG (Santa Cruz Biotechnology) was used as secondary antibody and bands were visualized using the ECL-Plus chemiluminescence detection system (Amersham). Autoradiograms were analyzed by densitometric analysis (Scion Image). GAPDH was used as loading control for P-p90RSK immunoblots and total NHE-1 (detected with a different polyclonal antibody from that used to immunoprecipitate samples) was used as the loading control for P-14-3-3 BM determinations.

Isolation of total RNA and real-time PCR

Quantitative PCR (qPCR) to measure NHE-1 mRNA abundance was performed using the real-time SYBR Green PCR method. Total RNA was isolated using RNeasy Mini Kit and RNase free Dnase Set (Qiagen) and reverse-transcribed using Omniscript RT Kit (Qiagen) as previously described [21]. The primers used were as follow: GAPDH forward primer 5′- CATGGCCTTCCGTGTTCCTA-3′ reverse primer 5′-TGCTTCACCACCTTCTTGATG-3′ NHE-1 forward primer 5′-CCCTCACGTGCGCACACCC-3′ reverse primer 5′-GACGTCTGATTGCAGGAAGG-3′. PCR reactions were performed with TaqDNA polymerase (Invitrogen). Fluorescence data were acquired at the end of extension. The cycle threshold value was measured and calculated by computer software (iCycler IQ OSS, version 3.0a, Bio-Rad). The cycle threshold value for NHE-1 was normalized by that for GAPDH in the same sample. For each experiment of real-time RT-PCR we obtained a melting curve of the amplified gene where it could be appreciated that only a specific product was amplified in each case with no primer–dimer formation.

We used 0.8 μg of total RNA to perform each RT. A 1:10 dilution in RNase free water of the cDNA obtained in the RT reaction (20 μl total volume) 5 μl were used in each qPCR.

The length of qPCR products was 101 bp for GAPDH and 193 bp for NHE-1.

Statistics

Data are expressed as mean±SEM. One-way ANOVA followed by Student–Newman–Keuls were used as appropriate. A $p<0.05$ value was considered significant.

Results

TAC produced ~45% increase in heart weight/body weight ratio compared to sham mice after 7 weeks; LOS partially prevented this hypertrophy, as shown in Table 1. The increased LV mass seen in TAC mice correlated with increased myocyte CSA and CVF, effects that were both reduced by LOS (Table 1). Representative photomicro-

Table 1 Indices of cardiac hypertrophy

	HW/BW	CSA (μm^2)	CVF (%)
Sham (n=8)	3.76±0.12	199.02±7.83	1.95±0.1
TAC (n=7)	5.58±0.30*	279.68±3.42*	5.62±0.4*
TAC+LOS (n=8)	4.43±0.10*$^{\#}$	215.50±4.57$^{\#}$	3.34±0.4*$^{\#}$

Heart weight/body weight ratio (HW/BW), myocyte cross-sectional area (CSA) and LV collagen volume fraction (CVF) in sham, TAC and TAC+LOS groups. TAC promoted cardiac hypertrophy, detected by the increase in HW/BW ratio, CSA, and CVF. LOS reduced cardiac hypertrophy and CVF (note that the changes induced by LOS are pressure-independent)

*$p<0.05$ vs. sham; $^{\#}p<0.05$ vs. TAC

graphs of LV sections from the three experimental groups are shown in Fig. 1. At the dose used herein, LV systolic pressures between both groups (TAC and TAC+LOS) were similar 3 days after TAC (128.6±5.4 vs. 128±3 mmHg, TAC and TAC+LOS, respectively), and at the end of the 7-week period (135±6.9 vs. 136±3 mmHg for TAC and TAC+LOS, respectively). Also, TAC did not change the aortic pressure distally to the coarctation (Table 2). These data validate the previous work of Rockman et al. [43] using the same model we used, and in addition show that arterial pressure proximal and distal to the constriction was not significantly altered by TAC in LOS-treated animals, suggesting that the hypertrophic regression was a direct effect of the AT1R blockade rather than a hemodynamic consequence.

Figure 2a shows representative echocardiographic images from sham, TAC and TAC+LOS mice. LV end-diastolic dimension, end-systolic dimension, wall thickness, endocardial fractional shortening and ejection fraction were calculated and shown in Fig. 2b. Compared to sham, TAC hearts had an increase in LV wall thickness of ~30%. LV end-diastolic dimension tended to increase in TAC mice, but this difference was not statistically significant. LV end-systolic dimension did increase in the TAC group, accounting for the decreased endocardial fractional shortening and ejection fraction seen in this group. Compared to non-treated rodents, and despite having less hypertrophy and identical LV systolic pressures, cardiac function was restored in mice treated with LOS, disputing in this case the concept of "compensatory hypertrophy."

In a separate group of sham-operated animals treated with the same dose of LOS, endocardial shortening did not change after 7 weeks (61.2±1.5% vs. 62.8±0.94%, Sham and Sham+LOS, respectively). Furthermore, heart weight/body weight was not significantly different between sham and sham+LOS (3.76±0.12 vs. 3.56±0.10 mg/g).

We next decided to evaluate LV function more extensively. By integrating LV pressures and dimensions, LV wall stress was calculated in all three groups as previously reported [20]. Wall stress is a composite parameter that

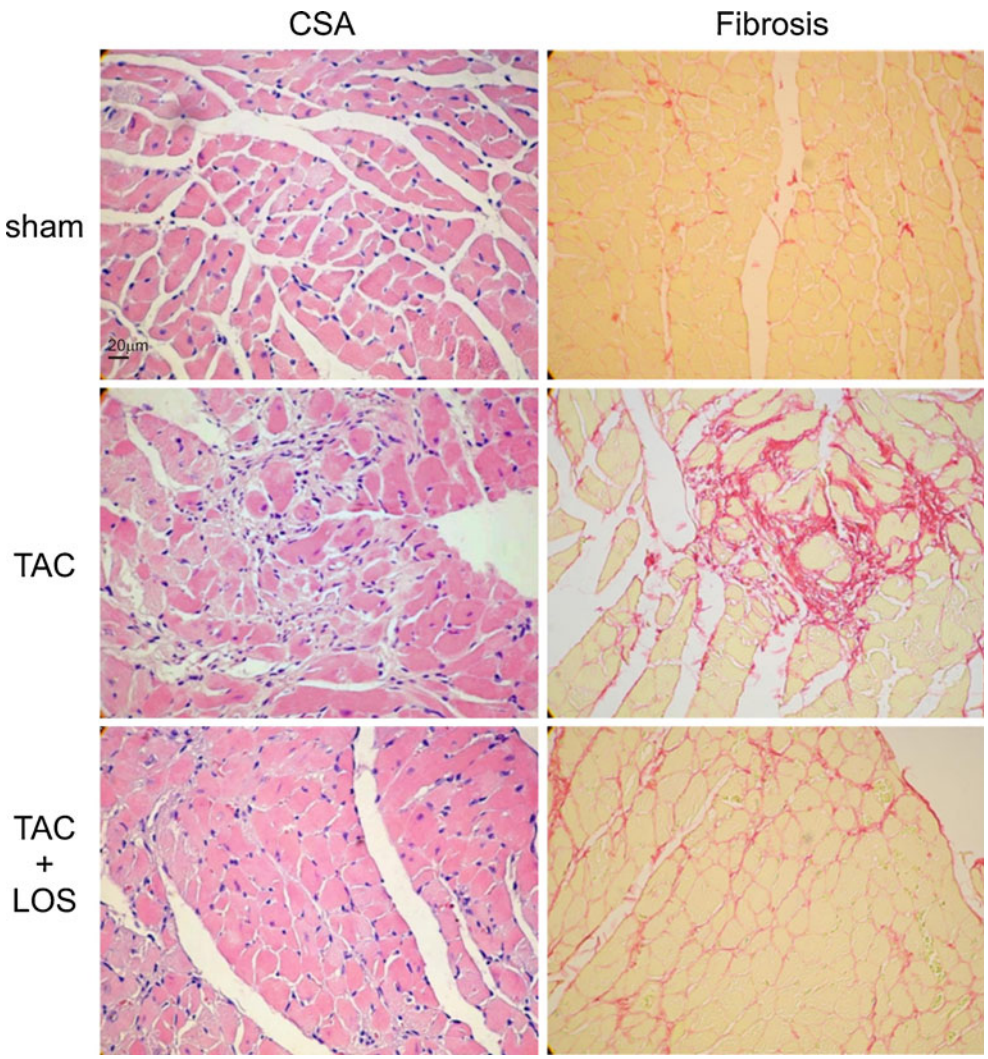

Fig. 1 Representative photomicrographs (×40 magnification) of left ventricular sections from sham, TAC and TAC+LOS groups. TAC increased myocyte cross-sectional area (*CSA*) and fibrosis; both effects were blunted by LOS

Table 2 Aortic pressure

	Proximal aortic pressure (mmHg)			Distal aortic pressure (mmHg)		
	Systolic BP	Diastolic BP	Mean BP	Systolic BP	Diastolic BP	Mean BP
Sham (n=4)	99±4	57±3	71±2	–	–	–
TAC (n=3)	138±6 #	64±4	88.6±3	91±5	54±3	66.3±2

Systolic, diastolic, and mean aortic blood pressure (BP) recorded in sham and mice subjected to TAC. Pressures did not significantly dropped in the aorta distal to the constriction, and the latter were similar to systemic aortic pressures in sham-operated animals

#p<0.02 vs. sham

includes LV pressure, radius of the cavity and thickness of its wall, and reflects the afterload imposed to the heart. Figure 3 shows LV end-diastolic pressure (LVEDP), together with end-systolic, peak-systolic and end-diastolic stress. A significant increase in LVEDP was observed after 7 weeks of TAC. LOS treatment modestly lowered LVEDP, but this difference was not statistically significant. As a result of the observed increase in LV wall thickness, peak and end-systolic stress decreased with TAC. These parameters were both normalized with LOS. Since in our model preload remained unchanged between treated and untreated groups (similar LVEDP and volumes), and systolic stress (afterload) increased (rather than decreased) in the TAC+LOS group, the increased endocardial fractional shortening seen in the LOS-treated animals truly reflects an increase in cardiac systolic performance.

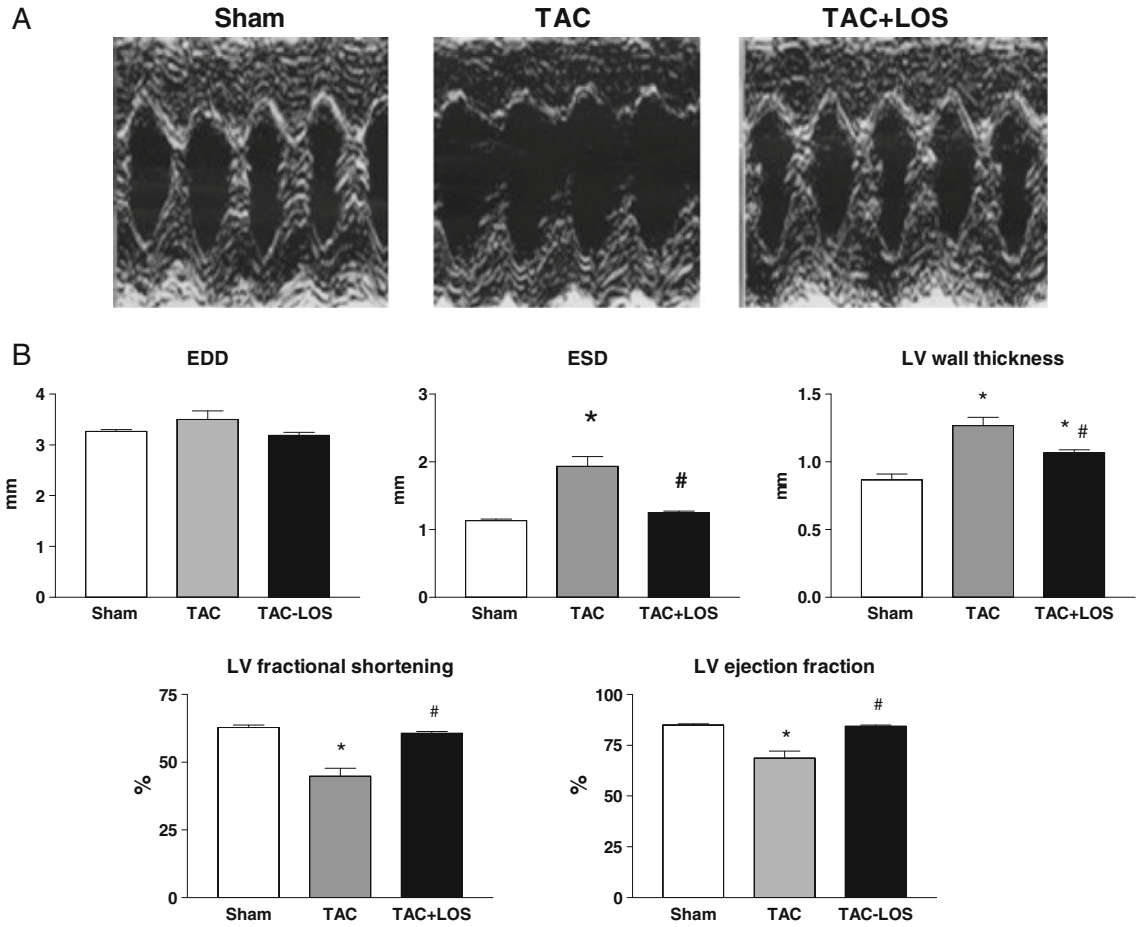

Fig. 2 **a** Representative echocardiograms obtained at the end of the experimental protocol (7 weeks) in sham, TAC and TAC+LOS mice. TAC mice showed depressed systolic function. This was prevented in TAC+LOS animals. **b** Overall results for end-diastolic and systolic dimensions (*EDD*, *ESD*), wall thickness, endocardial left ventricular (*LV*) fractional shortening and ejection fraction. TAC depressed both, LV fractional shortening and ejection fraction, and increased LV wall thickness. LOS ameliorated these indices. *p<0.05 vs. sham; #p<0.05 vs. TAC. n=6 in each group

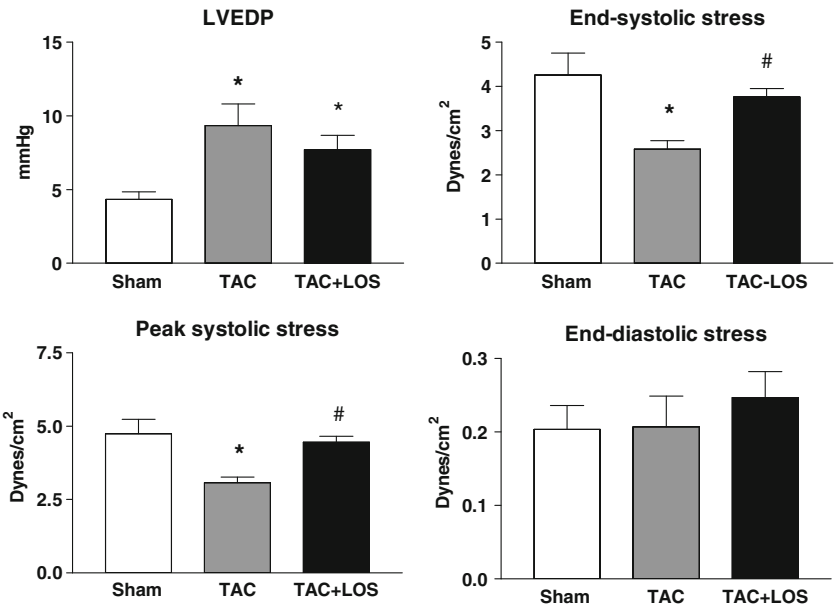

Fig. 3 Left ventricular end-diastolic pressure (*LVEDP*) was elevated after TAC, and LOS tended to normalize it, but the difference was not significant. TAC reduced, and LOS normalized both, end-systolic stress (*ESS*) and peak systolic stress (*PSS*). No significant changes were seen in end-diastolic stress (*EDS*) between groups. *$p<0.05$ vs. sham, #$p<0.05$ vs. TAC

It is evident from our data that the signals activated by TAC promoted a hypertrophic response that overcorrected LV wall stress. This "inappropriate hypertrophy," as described by de Simone et al. [18], was blunted by LOS; indeed, mice treated with the AT1R blocker only developed a small hypertrophic response, which sufficed to normalize systolic stress.

Next, in order to assess load-independent indices of cardiac performance, cardiac pressure–volume hemodynamic analysis was performed. Figure 4a depicts typical LV pressure–volume loops from sham, TAC and TAC+LOS mice. TAC displaced the end-systolic pressure volume relation (ESPVR) to the right and downward reflecting decreased systolic function. This was restored with LOS treatment. Figure 4b shows dP/dt_{max} corrected by LV radius/thickness. Since dP/dt_{max}, a traditional systolic contractile index, is known to augment proportionally as concentric hypertrophy increases, we corrected it by LV radius/thickness, as it has been previously proposed by Gleason and Braunwald [25] and by Carabello [10]. Once again, the fact that this index rose after decreasing CH in spite of increased wall stress, reflects enhanced systolic performance in LOS-treated animals. From the pressure–volume loops, end-diastolic pressure–volume relation was also determined, and by calculating the slope (β coefficient) of its monoexponential fit, LV end-diastolic stiffness was calculated. As depicted in Fig. 4c, TAC hearts showed increased stiffness. LOS tended to normalized this index (decreased stiffness), but as in the case of LVEDP, the difference was not statistically significant.

The critical role played by NHE-1 hyperactivity in pathological CH and failure has been recognized [3, 12, 40], and the redox-sensitive $p90^{RSK}$ is one of the main kinases involved in NHE-1 activation [16]; thus, we next decided to explore whether this pathway was activated in our model, and if it could be blocked by inhibiting AT1R.

Since LOS has been shown to interfere with ROS production [15, 23], we first determined lipid peroxidation by TBARS as an index of oxidative stress. Plasma TBARS were elevated in TAC mice and normalized after LOS treatment as shown in Fig. 5a.

Next, since oxidative stress is known to favor $p90^{RSK}$ activation, P-$p90^{RSK}$ was measured by immunoblot using a specific antibody. As shown in Fig. 5b, an increase in P-$p90^{RSK}$ was detected in the myocardium of mice subjected to TAC, while this was prevented in TAC animals treated with the AT1R blocker. Once activated, $p90^{RSK}$ phosphorylates NHE-1 at Ser703, creating a binding site for 14-3-3 proteins. Consistent with our $p90^{RSK}$ phosphorylation results, we assayed an antibody against P-14-3-3 binding motif in NHE-1 immunoprecipitates, and found a significantly higher signal indicative of enhanced NHE-1 activity in the hypertrophied myocardium of TAC mice, which was prevented with LOS (Fig. 5c). We also explored whether NHE-1 enhanced phosphorylation was accompanied by increased exchanger expression. To this aim, NHE-1 mRNA level was measured and, as shown in Fig. 5d, no difference in its abundance among the experimental groups was observed. This is consistent with what has been described in other models of CH, where hyperactivity of the exchanger, rather than its abundance, seems to be required to induce hypertrophy [17, 48, 56].

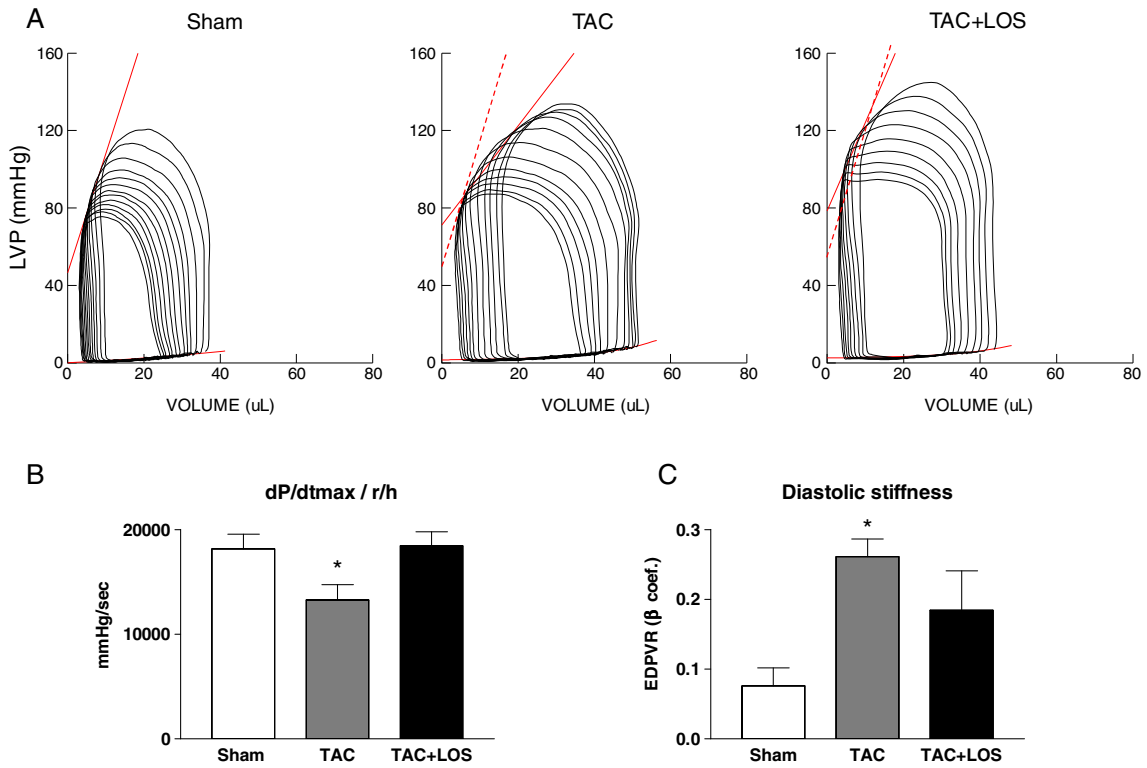

Fig. 4 **a** Representative cardiac pressure volume loops from a sham, TAC and TAC+LOS mouse. Compared to sham, TAC decreased cardiac systolic function, as reflected by a shift to the right of the normal end-systolic pressure volume relation (*ESPVR*) obtained in sham animals (*break line*). LOS restored ESPVR to the left. **b** dP/dt_{max} corrected to chamber concentricity (LV radius (*r*)/thickness (*h*)) also decreased with TAC and was restored with LOS. **c** TAC increased diastolic stiffness estimated as the slope of the end-diastolic pressure-volume relations (*EDPVR*). LOS tended to restore this index, but the difference was not statistically significant. *$p<0.05$ vs. sham. $n=6$ in each group

Discussion

The fact that ROS play an important role in determining pathological CH is a well-validated concept [2, 28]. Redox-sensitive mechanisms mediate CH in response to either pressure overload or other stimuli such as AII, α adrenergic agonists, tumor necrotic factor α, endothelin and mechanical stretch [28, 39, 54]. In this report, we provide in vivo evidence in favor of a redox-mediated NHE-1 activation as a mechanism in determining inappropriate CH, as it was previously suggested from in vitro experiments [52]. However, the possibility of alternate redox-sensitive mechanisms leading to CH by routes other than NHE-1 activation should also be considered [35].

Enhanced activity of the NHE-1 has been reported in genetic models of hypertensive CH, such as spontaneously hypertensive rats [41]. Although a hyperactive exchanger does not modify steady-state intracellular pH (because of compensatory bicarbonate dependent mechanisms) [41], it increases intracellular Na^+ with the consequent rise in Ca^{2+} through the Na^+/Ca^{2+} exchanger, leading to hypertrophic signals. As was pointed out in a recent work by Nakamura et al. [40], NHE-1 activation in myocytes transfected with hyperactive NHE-1 units seems to be sufficient to generate Ca^{2+} signals leading to CH. Furthermore, it has been reported that increased Ca^{2+} can also stimulates NHE-1 [34], generating a sort of vicious circle.

One of the earliest intracellular signals that follow myocardial stretch is the autocrine/paracrine release of AII and endothelin-1 (ET-1) by cardiomyocytes, leading to NHE-1 activation [13]. The seminal papers by Sadoshima et al. [44], Ito et al. [26] and Yamazaki et al. [55] showed this phenomenon in rat neonatal cardiomyocytes. This chain of events is detected also after stretching papillary muscles [13]. In this regard, phosphorylation of NHE-1 at Ser703 by the upstream ROS-sensitive kinase $p90^{RSK}$ appears to be the post-translational mechanism responsible for NHE-1 enhanced function [9]. Interestingly, the same intracellular signal activation pattern, i.e., an increase in the redox sensitive kinase $p90^{RSK}$, was detected in vivo in the present study after 7 weeks of TAC. Chronic treatment with LOS prevented the increase in TBARS, phosphorylation of $p90^{RSK}$, the consequent NHE-1 phosphorylation, and also cardiac function deterioration. We would like to highlight

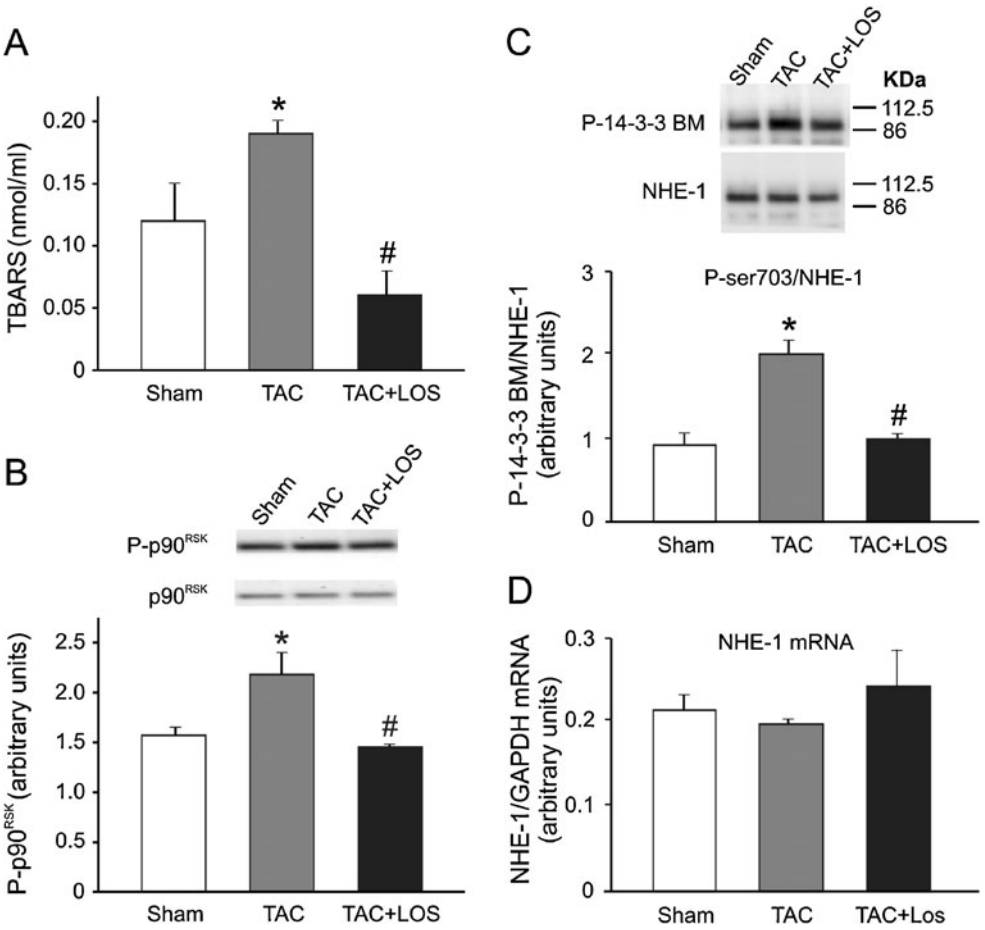

Fig. 5 **a** Lipid peroxidation estimated by plasma TBARS concentration increased in TAC mice and was normalized by LOS. **b** P-p90^{RSK} also showed a similar pattern. **c** Significant increase in NHE-1 phosphorylation at Ser703, estimated by a specific antibody against P-14-3-3 binding motif (*BM*), was detected in the hypertrophied myocardium of TAC-mice. This effect was prevented by LOS treatment. **d** Quantitative real time RT-PCR was used to determine NHE-1 mRNA abundance in each group. No difference in NHE-1 mRNA among groups was observed. *$p<0.05$ vs. sham; #$p<0.05$ vs. TAC. $n=7$ for sham, $n=8$ for TAC, $n=7$ for TAC+LOS

that plasma TBARS were proposed to be better indicators of oxidative stress than myocardial TBARS in the setting of CH [5].

The increased fibrosis accompanying CH seen in the present study was also diminished with LOS, similarly to what has been previously shown in the hypertrophic myocardium of spontaneously hypertensive rats undergoing chronic NHE-1 inhibition [14]. Interestingly, in the latter study, as well as in the present work, treatment did not decrease afterload. Several lines of evidence suggest that fibrosis development is linked to NOX activation and ROS production [6, 8]. In fact, cardiac fibrosis, induced either by AII or pressure overload, is significantly attenuated in NOX 2 knockout mice [6, 8]. In spite of the reduction in fibrosis seen with LOS, cardiac end-diastolic stiffness was not restored. It is possible that myocardial stiffness requires longer treatment time to normalize, or even that in that relative short term, LOS treatment did not affect the subtype of collagen or cross-link responsible for myocardial stiffness. Since we only measured total fibrosis, we were not able to differentiate them.

In our work, the origin of ROS or the isoform of NOX involved in the hypertrophic mechanism was not explored. However, previous in vitro experiments showed that mitochondria is the main source of NOX-dependent ROS formation after myocardial stretch [9] and that NOX 4 activity from mitochondrial origin [33] may play a role in addition to NOX 2 in CH development. Whether the recently described antioxidant properties of LOS [23] are playing a role beyond its direct AT1R inhibiting action was also not explored at the present time and deserves further investigation.

The reduction in wall thickness detected in LOS-treated vs. non-treated TAC hearts in the absence of changes in LV pressure or radius, determined an increase in LV wall stress. LOS did not restore wall thickness to control values (it remained ~24% higher than controls; Fig. 2), but certainly reduced it to levels "necessary" to counteract for the increase in pressure. In other words, the excessive CH was eliminated. It is interesting to note that in spite of the increase in wall stress seen with LOS, the reduction in CH seen with the AT1R blocker was accompanied by an increased cardiac performance, as reflected by the contractility indexes assessed not only by echocardiography but also by LV pressure–volume loops (Figs. 2 and 4). These findings could suggest that the amount of CH prevented by

LOS was maladaptive or "inappropriate," a concept coined by others [38]. In this regard, it seems that pressure overload may trigger multiple intracellular signaling pathways in addition to enhanced AT1R stimulation. Whereas some of these may be deleterious, others may benefit the heart, allowing it to adapt to different stressors. It is obvious that our data does not clarify whether or not the remnant hypertrophy seen herein was adaptive. Future experiments decreasing CH further and assessing cardiac performance will be necessary to elucidate this complex problem. As pointed out by Morisco et al. [36], the ideal therapeutic strategy towards hypertensive heart disease should aim to identify and target detrimental components while preserving beneficial ones. We could speculate that by preventing ROS production and NHE-1 phosphorylation we interfered with a pathway involved in the development of inappropriate maladaptive CH, not affecting the development of compensatory hypertrophy. Our hypothetical proposal is schematized in Fig. 6. Myocardial stretch induced by pressure overload triggers many intracellular signals. One of them, the autocrine/paracrine mechanism increases oxidative stress through the action of AII/ET-1 upon NOX, and leading to increase intracellular Na^+ and Ca^{2+} after NHE-1 activation. The AT1R inhibition prevented NOX activation and phosphorylation of $p90^{RSK}$ and NHE-1, decreasing the elevated Ca^{2+} levels and CH. At first glance, it appears difficult to explain the mechanisms by which a decrease in intracellular Ca^{2+} induced by NHE-1 inhibition can selectively diminish excessive CH without affecting the compensatory one. Baartscheer et al. [4], in experiments performed in rabbits, as we have likewise done [19] in cardiomyocytes isolated from neonatal rats, reported that NHE-1 inhibition decreased diastolic Ca^{2+} levels increasing the amplitude of the Ca^{2+} transient and thus improving myocardial contractility. We can speculate that the decrease in diastolic Ca^{2+} levels is the signal sensed by calcineurin and involved in maladaptive CH. On the other hand, compensatory hypertrophy would be triggered by mechanisms independent of diastolic Ca^{2+} levels or even by pathways not involving cytosolic Ca^{2+} at all. In connection with this, Wu et al. [53] showed that cardiomyocytes can distinguish simultaneous local and global Ca^{2+} signals involved in contractile activation from those targeting gene expression.

The question of why the elevation of $[Na^+]_i$ achieved by the NHE-1 is not corrected by the Na^+/K^+-ATPase activity may be raised. In this regard, Bers et al. [7] have shown that the amount in $[Na^+]_i$ necessary to alter the Na^+ pump activity is greater than those described to induce Ca^{2+} entry through the Na^+/Ca^{2+} exchanger.

Another point that deserves further comments is the impact that the coronary circulation might have on cardiac function in the setting of CH. In our model, proximal aortic pressures did not significantly changed between treated and untreated mice. Since LVEDP also did not significantly change, we also expect that differences in coronary perfusion pressure were minimal. However, we did not determine capillary density in heart tissue before and after CH, therefore, a difference in circulation at the capillary level with its consequences cannot be ruled out.

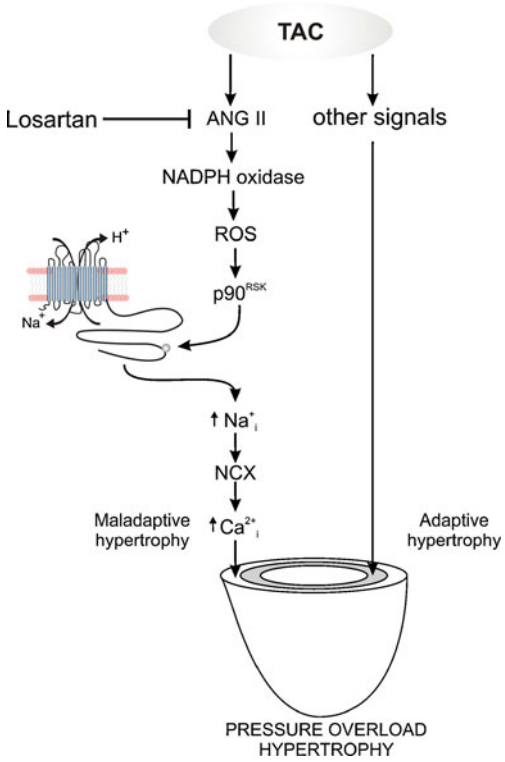

Fig. 6 Schematic representation of the proposed signaling pathway involved in the prevention of CH by AT1R blockade. In our scheme, the AT1R-sensitive part of the TAC-induced CH is maladaptive and related to redox-sensitive $p90^{RSK}$ activation, NHE-1 phosphorylation/activation, increase in intracellular Na^+ and the consequent increase in intracellular Ca^{2+} through the NCX. The increased Ca^{2+} concentration would then activate the calcineurin-NFAT signaling pathway responsible for triggering an abnormal cardiac growth. On the other hand, the same mechanical stimulus (stretch of cardiac muscle) may trigger other prohypertrophic signals intended to compensate for the increased wall stress ("adaptive hypertrophy") [11]. The reason for an improvement of cardiac performance accompanying the regression in CH due to AT1R blockade is not apparent to us at present. However, we could speculate about cancellation of the negative inotropic effect assigned to calcineurin phosphatase activation [30, 45]

In summary, in our model, TAC induced inappropriate CH, accompanied by ROS production and NHE-1 phosphorylation. AT1R blockade with LOS prevented redox-sensitive $p90^{RSK}$ activation and NHE-1 phosphorylation. The CH detected in TAC mice was deleterious, since cardiac performance decreased, and LOS prevented this as well. These experiments suggest for the first time an in vivo link between the AT1R blocker LOS, ROS-mediated NHE-1 phosphorylation and the development of CH, results that are online with previous in vitro experiments.

Acknowledgements We specially thank María Bracamonte and Georgina Luna for histological technical assistance. This work was supported in part by grants PICT 25475 and 01031 from Agencia Nacional de Promoción Científica of Argentina to Dr. HE Cingolani and Dr. NG Pérez, respectively, and PIP1386 from CONICET to Dr. NG Pérez.

Disclosures None.

References

1. Alvarez BV, Ennis IL, De Hurtado MC, Cingolani HE (2002) Effects of antihypertensive therapy on cardiac sodium/hydrogen ion exchanger activity and hypertrophy in spontaneously hypertensive rats. Can J Cardiol 18:667–672
2. Anilkumar N, Sirker A, Shah AM (2009) Redox sensitive signaling pathways in cardiac remodeling, hypertrophy and failure. Front Biosci 14:3168–3187
3. Baartscheer A, Hardziyenka M, Schumacher CA, Belterman CN, van Borren MM, Verkerk AO, Coronel R, Fiolet JW (2008) Chronic inhibition of the Na^+/H^+-exchanger causes regression of hypertrophy, heart failure, and ionic and electrophysiological remodelling. Br J Pharmacol 154:1266–1275
4. Baartscheer A, Schumacher CA, van Borren MM, Belterman CN, Coronel R, Opthof T, Fiolet JW (2005) Chronic inhibition of Na^+/H^+-exchanger attenuates cardiac hypertrophy and prevents cellular remodeling in heart failure. Cardiovasc Res 65:83–92
5. Baumer AT, Flesch M, Wang X, Shen Q, Feuerstein GZ, Bohm M (2000) Antioxidative enzymes in human hearts with idiopathic dilated cardiomyopathy. J Mol Cell Cardiol 32:121–130
6. Bendall JK, Cave AC, Heymes C, Gall N, Shah AM (2002) Pivotal role of a gp91(phox)-containing NADPH oxidase in angiotensin II-induced cardiac hypertrophy in mice. Circulation 105:293–296
7. Bers DM, Barry WH, Despa S (2003) Intracellular Na+regulation in cardiac myocytes. Cardiovasc Res 57:897–912
8. Byrne JA, Grieve DJ, Bendall JK, Li JM, Gove C, Lambeth JD, Cave AC, Shah AM (2003) Contrasting roles of NADPH oxidase isoforms in pressure-overload versus angiotensin II-induced cardiac hypertrophy. Circ Res 93:802–805
9. Caldiz CI, Garciarena CD, Dulce RA, Novaretto LP, Yeves AM, Ennis IL, Cingolani HE, Chiappe de Cingolani G, Perez NG (2007) Mitochondrial reactive oxygen species activate the slow force response to stretch in feline myocardium. J Physiol 584:895–905
10. Carabello BA (2002) Evolution of the study of left ventricular function: everything old is new again. Circulation 105:2701–2703
11. Catalucci D, Latronico MV, Ellingsen O, Condorelli G (2008) Physiological myocardial hypertrophy: how and why? Front Biosci 13:312–324
12. Cingolani HE, Ennis IL (2007) Sodium–hydrogen exchanger, cardiac overload, and myocardial hypertrophy. Circulation 115:1090–1100
13. Cingolani HE, Ennis IL, Aiello EA, Perez NG (2011) Role of autocrine/paracrine mechanisms in response to myocardial strain. Pflugers Arch 462:29–38
14. Cingolani HE, Rebolledo OR, Portiansky EL, Perez NG, Camilion de Hurtado MC (2003) Regression of hypertensive myocardial fibrosis by Na(+)/H(+) exchange inhibition. Hypertension 41:373–377
15. Costa LE, La-Padula P, Lores-Arnaiz S, D'Amico G, Boveris A, Kurnjek ML, Basso N (2002) Long-term angiotensin II inhibition increases mitochondrial nitric oxide synthase and not antioxidant enzyme activities in rat heart. J Hypertens 20:2487–2494
16. Cuello F, Snabaitis AK, Cohen MS, Taunton J, Avkiran M (2007) Evidence for direct regulation of myocardial Na^+/H^+ exchanger isoform 1 phosphorylation and activity by 90-kDa ribosomal S6 kinase (RSK): effects of the novel and specific RSK inhibitor fmk on responses to alpha1-adrenergic stimulation. Mol Pharmacol 71:799–806
17. Darmellah A, Baetz D, Prunier F, Tamareille S, Rucker-Martin C, Feuvray D (2007) Enhanced activity of the myocardial Na^+/H^+ exchanger contributes to left ventricular hypertrophy in the Goto–Kakizaki rat model of type 2 diabetes: critical role of Akt. Diabetologia 50:1335–1344
18. de Simone G, Devereux RB, Kimball TR, Mureddu GF, Roman MJ, Contaldo F, Daniels SR (1998) Interaction between body size and cardiac workload: influence on left ventricular mass during body growth and adulthood. Hypertension 31:1077–1082
19. Dulce RA, Hurtado C, Ennis IL, Garciarena CD, Alvarez MC, Caldiz C, Pierce GN, Portiansky EL, Chiappe de Cingolani GE, Camilion de Hurtado MC (2006) Endothelin-1 induced hypertrophic effect in neonatal rat cardiomyocytes: involvement of Na^+/H^+ and Na^+/Ca^{2+} exchangers. J Mol Cell Cardiol 41:807–815
20. Ennis IL, Escudero EM, Console GM, Camihort G, Dumm CG, Seidler RW, Camilion de Hurtado MC, Cingolani HE (2003) Regression of isoproterenol-induced cardiac hypertrophy by Na^+/H^+ exchanger inhibition. Hypertension 41:1324–1329
21. Ennis IL, Garciarena CD, Perez NG, Dulce RA, Camilion de Hurtado MC, Cingolani HE (2005) Endothelin isoforms and the response to myocardial stretch. Am J Physiol Heart Circ Physiol 288:H2925–H2930
22. Fanelli C, Zatz R (2011) Linking oxidative stress, the renin–angiotensin system, and hypertension. Hypertension 57:373–374
23. Fortuno A, Bidegain J, Robador PA, Hermida J, Lopez-Sagaseta J, Beloqui O, Diez J, Zalba G (2009) Losartan metabolite EXP3179 blocks NADPH oxidase-mediated superoxide production by inhibiting protein kinase C: potential clinical implications in hypertension. Hypertension 54:744–750
24. Fortuno MA, Ravassa S, Etayo JC, Diez J (1998) Overexpression of Bax protein and enhanced apoptosis in the left ventricle of spontaneously hypertensive rats: effects of AT1 blockade with losartan. Hypertension 32:280–286
25. Gleason WL, Braunwald E (1962) Studies on the first derivative of the ventricular pressure pulse in man. J Clin Invest 41:80–91
26. Ito H, Hirata Y, Adachi S, Tanaka M, Tsujino M, Koike A, Nogami A, Murumo F, Hiroe M (1993) Endothelin-1 is an autocrine/paracrine factor in the mechanism of angiotensin II-induced hypertrophy in cultured rat cardiomyocytes. J Clin Invest 92:398–403
27. Koren MJ, Devereux RB, Casale PN, Savage DD, Laragh JH (1991) Relation of left ventricular mass and geometry to morbidity and mortality in uncomplicated essential hypertension. Ann Intern Med 114:345–352
28. Kuroda J, Ago T, Matsushima S, Zhai P, Schneider MD, Sadoshima J (2010) NADPH oxidase 4 (Nox4) is a major source of oxidative stress in the failing heart. Proc Natl Acad Sci U S A 107:15565–15570
29. Lehoux S, Abe J, Florian JA, Berk BC (2001) 14-3-3 Binding to Na^+/H^+ exchanger isoform-1 is associated with serum-dependent activation of Na^+/H^+ exchange. J Biol Chem 276:15794–15800
30. Li J, Yatani A, Kim SJ, Takagi G, Irie K, Zhang Q, Karoor V, Hong C, Yang G, Sadoshima J, Depre C, Vatner DE, West MJ, Vatner SF (2003) Neurally-mediated increase in calcineurin activity regulates cardiac contractile function in absence of hypertrophy. Cardiovasc Res 59:649–657
31. Litwin SE, Katz SE, Weinberg EO, Lorell BH, Aurigemma GP, Douglas PS (1995) Serial echocardiographic-Doppler assessment of left ventricular geometry and function in rats with pressure-overload hypertrophy. Chronic angiotensin-converting enzyme

inhibition attenuates the transition to heart failure. Circulation 91:2642–2654
32. Lloyd-Jones DM, Larson MG, Leip EP, Beiser A, D'Agostino RB, Kannel WB, Murabito JM, Vasan RS, Benjamin EJ, Levy D (2002) Lifetime risk for developing congestive heart failure: the Framingham Heart Study. Circulation 106:3068–3072
33. Maejima Y, Kuroda J, Matsushima S, Ago T, Sadoshima J (2011) Regulation of myocardial growth and death by NADPH oxidase. J Mol Cell Cardiol 50:408–416
34. Maly K, Strese K, Kampfer S, Ueberall F, Baier G, Ghaffari-Tabrizi N, Grunicke HH, Leitges M (2002) Critical role of protein kinase C alpha and calcium in growth factor induced activation of the Na(+)/H(+) exchanger NHE1. FEBS Lett 521:205–210
35. Matsuzawa A, Ichijo H (2005) Stress-responsive protein kinases in redox-regulated apoptosis signaling. Antioxid Redox Signal 7:472–481
36. Morisco C, Sadoshima J, Trimarco B, Arora R, Vatner DE, Vatner SF (2003) Is treating cardiac hypertrophy salutary or detrimental: the two faces of Janus. Am J Physiol Heart Circ Physiol 284: H1043–H1047
37. Muiesan ML, Salvetti M, Rizzoni D, Castellano M, Donato F, Agabiti-Rosei E (1995) Association of change in left ventricular mass with prognosis during long-term antihypertensive treatment. J Hypertens 13:1091–1095
38. Mureddu GF, Cioffi G, Stefenelli C, Boccanelli A, de Simone G (2009) Compensatory or inappropriate left ventricular mass in different models of left ventricular pressure overload: comparison between patients with aortic stenosis and arterial hypertension. J Hypertens 27:642–649
39. Nakamura K, Fushimi K, Kouchi H, Mihara K, Miyazaki M, Ohe T, Namba M (1998) Inhibitory effects of antioxidants on neonatal rat cardiac myocyte hypertrophy induced by tumor necrosis factor-alpha and angiotensin II. Circulation 98:794–799
40. Nakamura TY, Iwata Y, Arai Y, Komamura K, Wakabayashi S (2008) Activation of Na^+/H^+ exchanger 1 is sufficient to generate Ca^{2+} signals that induce cardiac hypertrophy and heart failure. Circ Res 103:891–899
41. Perez NG, Alvarez BV, Camilion de Hurtado MC, Cingolani HE (1995) pHi regulation in myocardium of the spontaneously hypertensive rat. Compensated enhanced activity of the Na(+)-H+ exchanger. Circ Res 77:1192–1200
42. Perez NG, Piaggio MR, Ennis IL, Garciarena CD, Morales C, Escudero EM, Cingolani OH, Chiappe de Cingolani G, Yang XP, Cingolani HE (2007) Phosphodiesterase 5A inhibition induces Na^+/H^+ exchanger blockade and protection against myocardial infarction. Hypertension 49:1095–1103
43. Rockman HA, Wachhorst SP, Mao L, Ross J Jr (1994) ANG II receptor blockade prevents ventricular hypertrophy and ANF gene expression with pressure overload in mice. Am J Physiol 266: H2468–H2475
44. Sadoshima J, Xu Y, Slayter HS, Izumo S (1993) Autocrine release of angiotensin II mediates stretch-induced hypertrophy of cardiac myocytes in vitro. Cell 75:977–984
45. Sah R, Oudit GY, Nguyen TT, Lim HW, Wickenden AD, Wilson GJ, Molkentin JD, Backx PH (2002) Inhibition of calcineurin and sarcolemmal Ca^{2+} influx protects cardiac morphology and ventricular function in K(v)4.2 N transgenic mice. Circulation 105:1850–1856
46. Sahn DJ, DeMaria A, Kisslo J, Weyman A (1978) Recommendations regarding quantitation in M-mode echocardiography: results of a survey of echocardiographic measurements. Circulation 58:1072–1083
47. Samuel JL, Swynghedauw B (2008) Is cardiac hypertrophy a required compensatory mechanism in pressure-overloaded heart? J Hypertens 26:857–858
48. Schussheim AE, Radda GK (1995) Altered Na(+)-H(+)-exchange activity in the spontaneously hypertensive perfused rat heart. J Mol Cell Cardiol 27:1475–1481
49. Segers P, Georgakopoulos D, Afanasyeva M, Champion HC, Judge DP, Millar HD, Verdonck P, Kass DA, Stergiopulos N, Westerhof N (2005) Conductance catheter-based assessment of arterial input impedance, arterial function, and ventricular–vascular interaction in mice. Am J Physiol Heart Circ Physiol 288:H1157–H1164
50. Snabaitis AK, D'Mello R, Dashnyam S, Avkiran M (2006) A novel role for protein phosphatase 2A in receptor-mediated regulation of the cardiac sarcolemmal Na^+/H^+ exchanger NHE1. J Biol Chem 281:20252–20262
51. Takahashi E, Abe J, Gallis B, Aebersold R, Spring DJ, Krebs EG, Berk BC (1999) p90(RSK) is a serum-stimulated Na^+/H^+ exchanger isoform-1 kinase. Regulatory phosphorylation of serine 703 of Na^+/H^+ exchanger isoform-1. J Biol Chem 274:20206–20214
52. Takimoto E, Kass DA (2007) Role of oxidative stress in cardiac hypertrophy and remodeling. Hypertension 49:241–248
53. Wu X, Zhang T, Bossuyt J, Li X, McKinsey TA, Dedman JR, Olson EN, Chen J, Brown JH, Bers DM (2006) Local InsP3-dependent perinuclear Ca^{2+} signaling in cardiac myocyte excitation–transcription coupling. J Clin Invest 116:675–682
54. Xiao L, Pimentel DR, Wang J, Singh K, Colucci WS, Sawyer DB (2002) Role of reactive oxygen species and NAD(P)H oxidase in alpha(1)-adrenoceptor signaling in adult rat cardiac myocytes. Am J Physiol Cell Physiol 282:C926–C934
55. Yamazaki T, Komuro I, Kudoh S, Zou Y, Shiojima I, Hiroi Y, Mizuno T, Maemura K, Kurihara H, Aikawa R, Takano H, Yazaki Y (1996) Endothelin-1 is involved in mechanical stress-induced cardiomyocyte hypertrophy. J Biol Chem 271:3221–3228
56. Yokoyama H, Gunasegaram S, Harding SE, Avkiran M (2000) Sarcolemmal Na^+/H^+ exchanger activity and expression in human ventricular myocardium. J Am Coll Cardiol 36:534–540